Sediment preservation and accretion rates of fluvial meander-belt deposits: variations with temporal scale and river size

N. Yan[1]*, L. Colombera[1,2] and N. P. Mountney[1]

[1]Fluvial, Eolian & Shallow-Marine Research Group, School of Earth and Environment, University of Leeds, Leeds LS2 9JT, UK

[2]Department of Earth and Environmental Sciences, Università di Pavia, Via Ferrata 1, 27100 Pavia, Italy

NY, 0000-0003-1790-5861; LC, 0000-0001-9116-1800; NPM, 0000-0002-8356-9889
*Correspondence: n.yan@leeds.ac.uk

Abstract: The preservation and accretion rates of fluvial meander-belt deposits appear to vary with the time over which they are evaluated, but the drivers of this effect are not fully understood. Using channel trajectories tracking the temporal evolution of meandering rivers, constrained with data on past river planforms, a numerical model is used to simulate planform evolutions of meander-belt reaches that underwent different types of meander transformation behaviours and bend cutoffs. Sediment preservation and bar accretion rates are quantified for three hierarchies of depositional products: (i) accretion stages reflecting intervals of bend migration by a certain meander-transformation style, (ii) meander-belt segments encompassing multiple stages but no bend cutoffs and (iii) meander-belt segments that experienced one or multiple cutoffs. Results show that distinct power-law relationships between the accretion rate and the time of sedimentation exist for river systems of different magnitudes in scale. Within each order of magnitude in river-system size, a single power-law relationship fails to effectively capture all depositional hierarchies. Sediment preservation varies with the time over which it is computed, but systematic variations in accretion rates with time primarily portray an apparent dependency of river migration rates on time: these variations largely reflect the temporal resolution and timespan of the modelled examples, highlighting an inherent issue affecting studies of river evolutions.

The accretion of fluvial point bars and of the larger meander belts they form is locally episodic and punctuated by interludes of bar erosion (Barrell 1917; Ager 1993; Dott 1996; Miall 2015). The episodic nature of depositional and erosional processes gives rise to time gaps in the preserved depositional products of bank accretion, in a manner whereby the duration of gaps in the sedimentary record tends to increase, on average, with the overall length of time (Durkin *et al.* 2018; Yan *et al.* 2021*a*). As a result, average sediment accumulation rates tend to decrease with the time span over which they are determined. This phenomenon is known as the 'Sadler effect' and is described by a negative power-law relationship between sediment accumulation rates and time (Sadler 1981). In fluvial meandering rivers, sediment accumulation partly takes place by lateral accretion of migrating channels, at rates that are usually orders of magnitude greater than the rate of vertical aggradation. Lateral accretion rates are intimately related to sediment preservation, which in meander-belt deposits is inherently linked to channel morphodynamics. The amount and spatial distribution of sediment erosion and accumulation, and the resulting sediment preservation, are related to meander-bend transformation behaviours (Ghinassi *et al.* 2016; Durkin *et al.* 2018). The point bars of expansional meanders tend to grow laterally, approximately perpendicularly to the channel-belt direction. By contrast, the point bars of downstream-translating bends dominantly accrete downriver, for example because of lateral confinement by valley walls (Ghinassi and Ielpi 2015) or the presence of an erosion-resistant substrate, such as mud-prone abandoned channel fills (Smith *et al.* 2009; Labrecque *et al.* 2011). As a result, at the timescale of appreciable migration, the point bars of translating bends experience near-constant erosion and reworking of their bar-head regions (Smith *et al.* 2009, 2011; Ghinassi *et al.* 2014, 2016; Ielpi and Ghinassi 2014). Furthermore, intra-channel-belt erosion can locally occur due to the progressive or episodic rotation of meander bends (Ielpi and Ghinassi 2014; Yan *et al.* 2021*b*). Relatively mature fluvial meanders can evolve through numerous distinct stages of bar growth, each of which may be characterized by different directions of channel migration, different styles of meander transformations and various

From: Finotello, A., Durkin, P. R. and Sylvester, Z. (eds) *Meandering Streamflows: Patterns and Processes across Landscapes and Scales*. Geological Society, London, Special Publications, **540**, https://doi.org/10.1144/SP540-2022-142

degrees of bend-apex rotation (Daniel 1971; Ghinassi *et al.* 2016; Durkin *et al.* 2018; Hagstrom *et al.* 2019). Later stages of bar evolution commonly encompass episodes of partial erosion of bar deposits accumulated during earlier stages, thereby resulting in the development of complex mosaics of accretion patterns that are evident as scroll-bar morphologies in the planforms of modern fluvial channel belts (Strick *et al.* 2018; Durkin *et al.* 2019; Johnston and Holbrook 2019; Russell *et al.* 2019; Willis and Sech 2019; Yan *et al.* 2021*a*, *b*). Processes of neck- or chute-cutoff can cause significant erosion of bar deposits, as well as the establishment of new channel courses that may differ in morphodynamic behaviour (Hooke 1995; Schwenk and Foufoula-Georgiou 2016; Viero *et al.* 2018). These processes occur at different temporal and spatial scales, and collectively determine the stratigraphic completeness of meander-belt deposits. These processes also establish temporal and spatial thresholds that govern sediment preservation and planform accumulation rates. Durkin *et al.* (2018) quantified the 'stratigraphic completeness' (Sadler and Strauss 1990) of meander-belt deposits as the fraction of time recorded in the stratigraphy, and found that sediment preservation of fluvial meander-belt deposits decays with time logarithmically. Yan *et al.* (2021*a*) assessed the degree to which a Sadler-type effect in meander-belt accretion rates is expressed across different hierarchies of channel-belt deposits; this was done by applying a numerical modelling tool called the Point-Bar Sedimentary Architecture Numerical Deduction (PB-SAND; Yan *et al.* 2017), to simulate the recent evolution of modern meander-belt reaches, all normalized in scale relative to a fixed river-channel width. This approach allowed Yan *et al.* (2021*a*) to simulate scale-free meandering rivers, constrained using time-lapse trajectories of natural examples, and employing proxies for temporal duration that are essentially based on the area over which the modelled rivers migrated. By utilizing this approach, these authors recognized that the relationship between planform accretion rates and time is not well described by a simple power-law decay (Yan *et al.* 2021*a*), as generally observed for the vertical accumulation rates of the broader range of hierarchies of fluvial strata (Sadler 1981; Pelletier and Turcotte 1997). Rather, more complicated relationships between time and accretion rates may be attributed to the onset of geomorphic thresholds of channel transformations and cutoffs (Yan *et al.* 2021*a*). Notwithstanding, the findings of Yan *et al.* (2021*a*) still require corroboration with datasets associated with independent measures of time, to shed light on whether the observed relationships between accretion rates and their surrogate measure of time persist in datasets for which real temporal durations can be constrained. Furthermore, as prevailing geomorphic processes vary at different temporal and spatial scales (Lawler 1993; Couper 2004), the relationships between time and accretion rates are likely to vary with the river scale for different hierarchies of fluvial deposits. To this end, the aim of this study is to examine the relationships between sediment preservation, accretion rate and the time span over which these quantities are determined. The temporal scales of meander-belt examples are constrained based on former river channel positions identified from historical maps and remote-sensing datasets (e.g. aerial photographs, satellite images), and with consideration of the physical scale of the river systems. By these means, the morphodynamic controls on the preservation of fluvial meander-belt deposits discussed in Yan *et al.* (2021*a*) are assessed further.

Methodology

The PB-SAND (Yan *et al.* 2017, 2021*a*, *b*), is a forward stratigraphic model that can be employed to simulate the planform evolution and sedimentary architecture of meander belts given a set of channel trajectories whose time of development is known. These control trajectories are selected based on the growth behaviours of meander belts and bar transformation styles and can be digitized from historical maps, aerial photographs, satellite images or seismic-reflection time or stratal slices in the case of ancient subsurface successions (e.g. t_1–t_5 in Fig. 1a). The shape of each input trajectory is captured by a user-specified number of control points. Bar accretions between two consecutive control trajectories are obtained by linear interpolation between control points at these times, based on a specified number of time steps. Planform point-bar accretion is modelled as taking place over the area enclosed by two consecutive trajectories. Erosion occurs when older meander-belt areas are subsequently overprinted by the mobile channel thread.

In this study, the evolutions of 15 meander-belt examples, from rivers of variable sizes, have been modelled across temporal scales of decades to thousands of years. This has been possible thanks to data on historical channel trajectories tracking river migration, drawn from the scientific literature, historical maps and satellite images (Table 1). These chosen examples cover a range of river scales, meander transformation styles and frequencies of bend cut-offs. All case examples are informed by input trajectories depicting the centrelines of river channels at known times, obtained from publicly available historical maps or satellite images. Accretion steps intervening between two temporally consecutive input trajectories are modelled by linear interpolation

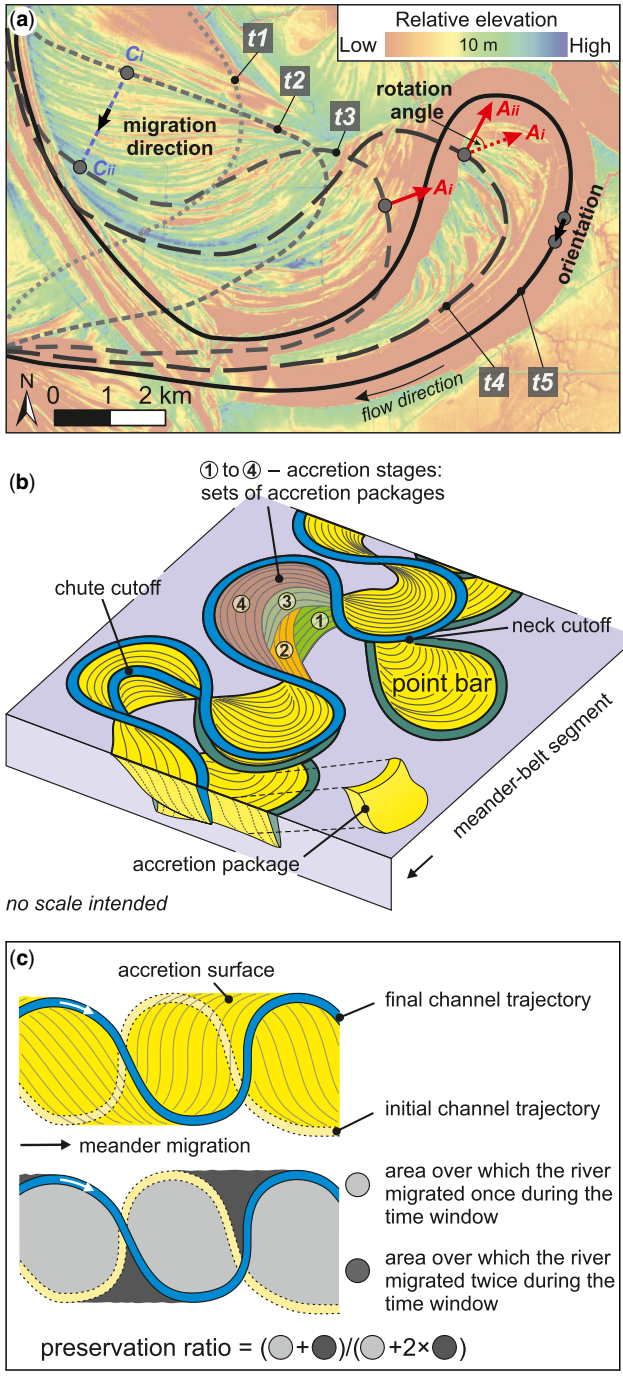

Fig. 1. Illustration of methods and quantifications. (**a**) Example of input trajectories digitized from a LiDAR image of a point-bar from the Mississippi River. t_1 to t_5 denote chronological order. '*C*' and '*A*' denote a control point and a meander apex, respectively. Vector connecting *Ci* to *Cii* denotes the migration direction of the control point over two time steps. Angle between *Ai* and *Aii* denotes the degree of apex rotation over two time steps. (**b**) Hierarchies of sedimentary architecture considered here: accretion packages, accretion stages and meander-belt segments. (**c**) Definition of sediment preservation ratio.

Table 1. *Location of the 15 considered meander-belt examples, for which time-lapse river trajectories were recorded in the literature or extracted from satellite images in Google Earth*

Planform ID	Latitude	Longitude	Location	Duration modelled (years)	Channel trajectories and temporal constraints
1	53°19′15.70″N	2°11′17.08″W	River Bollin, UK	67	Hooke (2004)
2	53°19′17.62″N	2°11′12.55″W	River Bollin, UK	67	Hooke (2004)
3	53°11′1.47″N	2°15′32.81″W	River Dane, UK	23	Hooke and Yorke (2010)
4	53°10′57.63″N	2°15′32.47″W	River Dane, UK	23	Hooke and Yorke (2010)
5	53°11′25.79″N	2°16′53.73″W	River Dane, UK	23	Hooke and Yorke (2010)
6	52°32′19.57″N	6°28′21.57″E	Overijsselse Vecht, Germany	180	Quik and Wallinga (2018)
7	52°30′25.50″N	6°30′26.24″E	Overijsselse Vecht, Germany	114	Quik and Wallinga (2018)
8	14° 2′13.96″S	65° 5′55.62″W	Mamoré River, Bolivia	30	Sylvester *et al.* (2021)
9	48°55′6.23″N	17°16′29.51″E	Morava River, Czech Republic	74	Ondruch and Máčka (2015)
10	7°52′27.28″S	74°47′55.04″W	Ucayali River, Peru	36	Google Earth
11	7°55′37.52″S	74°42′31.36″W	Ucayali River, Peru	36	Google Earth
12	7°37′14.59″S	75° 2′29.88″W	Ucayali River, Peru	36	Google Earth
13	9°13′26.85″S	74°22′52.70″W	Ucayali River, Peru	36	Google Earth
14	9°33′40.24″S	74°11′30.33″W	Ucayali River, Peru	25	Walcker *et al.* (2021)
15	61°48′24.68″N	51°42′10.21″E	Vychegda River, Russia	3500	Karmanov *et al.* (2013)

of the change in position of the channel centreline. The number of accretion increments between two consecutive input trajectories is chosen based on visual evaluation of accretion patterns shown in planform in the form of scroll morphologies. The length of time of successive accretion increments between two consecutive interpolated accretion trajectories is considered constant in the same meander-belt case. The time increment associated with each pair of consecutive accretion steps determines the temporal resolution at which point-bar cannibalization is captured (Yan *et al.* 2017). An example of a modelled channel belt is shown in Figure 2. The time of development of each input channel centreline is shown for all meander-belt examples in Figure 3 (as year AD). Meander-belt examples that cover longer temporal evolutions are generally characterized by coarser temporal resolution, meaning that the average duration of sets of accretion steps bounded by successive input centrelines ('stages', see below) tends to be larger. The modelled channel width is set as equal to the width of the present-day channel, as observed at the flow stage for which data are available in the literature or observations from remote sensing were made; this means that the employed width data may refer to channels at different flow stages, dependent on the exact time of record.

The modelling outputs are used to quantify sediment preservation for three hierarchies of sedimentary products (Fig. 1b): (i) sets of accretion packages representing the preserved expression of different stages of bar evolution characterized by different meander migration styles and amounts of bend-apex rotation (termed 'stages' hereafter), (ii), meander-belt segments without bend cutoffs, containing multiple sets of accretion packages, which may be dominated by different styles of meander transformations and (iii) meander-belt segments with one or multiple bend cutoffs. The preservation of meander-belt deposits is calculated accounting for the erosion and deposition of accretion packages bounded by consecutive accretion surfaces. The 'preservation ratio' provides a measure of the fraction of meander-belt deposits that are preserved over a given temporal scale. The 'preservation ratio' is defined here as the ratio between the planform area covered by deposits accumulated over a certain length of time that are preserved at the end of that time window (area of net deposition) and the total area over which the river has wandered over the same time episode (area of river migration), regardless of whether some parts have later been eroded (Fig. 1c). Therefore, the preservation of channel-belt deposits is only based on the erosion and deposition occurring during the time interval in

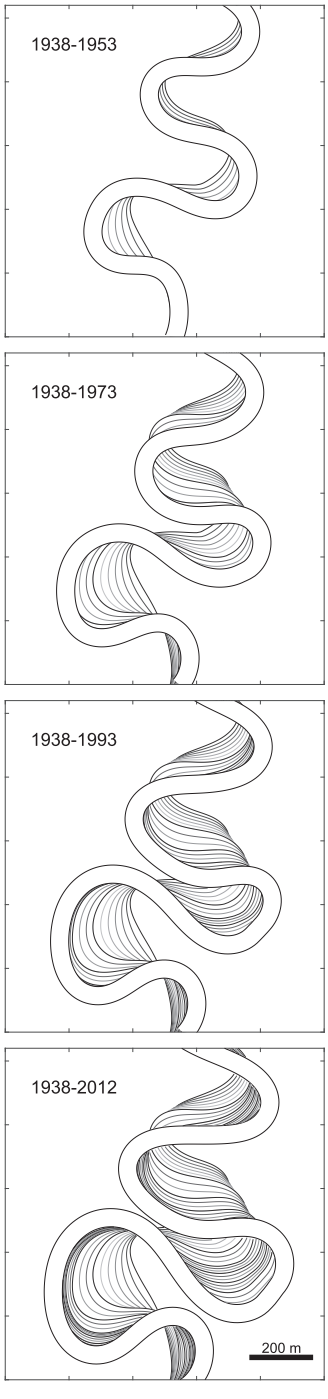

Fig. 2. Planform evolution of the meander belt of the Morava River (case *CB_9*) modelled by PB-SAND. Eight input trajectories (corresponding to river positions in 1938, 1953, 1963, 1973, 1982, 1993, 2003 and 2012) are digitized based on the reconstruction by Ondruch and Mácka (2015).

question; the erosion of older packages is not taken into account, in contrast with the 'survivability curves' of Durkin *et al.* (2018). The migration rate is defined as the ratio between the area of river migration per channel length and the temporal duration. The accretion rate is defined as the ratio between the area of net deposition per channel length and the temporal duration. Thus, the bar accretion rate is smaller than (or equal to, if no erosion takes place) the corresponding migration rate. As the calculations of the migration rate and the accretion rate are based on the channel centrelines, changes of channel width are not considered.

The planform characteristics of each hierarchy of architectural products are analysed by considering channel sinuosity, a quantity termed 'migration angle' and meander-apex rotation (Fig. 1a). The channel sinuosity is calculated as the ratio between the streamwise length and the straight distance between the two end points of each modelled channel trajectory (Friend and Sinha 1993). The migration angle of each accretion package is defined as the absolute angle (domain: 0–180°) between the direction of channel migration and the channel-belt orientation. The direction of channel migration is estimated based on the direction of shift of corresponding control points across two consecutive trajectories, and the channel-belt orientation is approximated by the circular mean of downstream channel direction, that is, the vector mean of the direction of lines connecting two consecutive control points along the river-flow direction. As measures of temporal variability in point-bar accretion styles at two different hierarchical orders, the following quantities are computed: (i) the circular standard deviation of the migration angle of each time step within each bar accretion stage; and (ii) the circular standard deviation of the migration-angle circular mean of each accretion stage within each meander-belt segment. The circular standard deviation is defined as $\sqrt{-2\ln(R)}$ where R is the mean resultant length. The degree of rotation of each meander is defined as the change of direction of the meander apex across two consecutive accretion packages, where the meander apex is the point of local maximum bend curvature between two channel inflection points (Yan *et al.* 2021*b*).

This study is subject to some limitations. The number of studied natural meander belts is relatively limited, especially for examples recording multiple cut-off events. There exist only a limited number of rivers for which detailed and reliable records of historical channel positions are known. Sediment preservation of meander belts is estimated based on 2D planform areas (cf. Durkin *et al.* 2018), rather than 3D sediment volumes, for ease of computation. Thus, meander-belt thickness variations that reflect temporal and streamwise changes

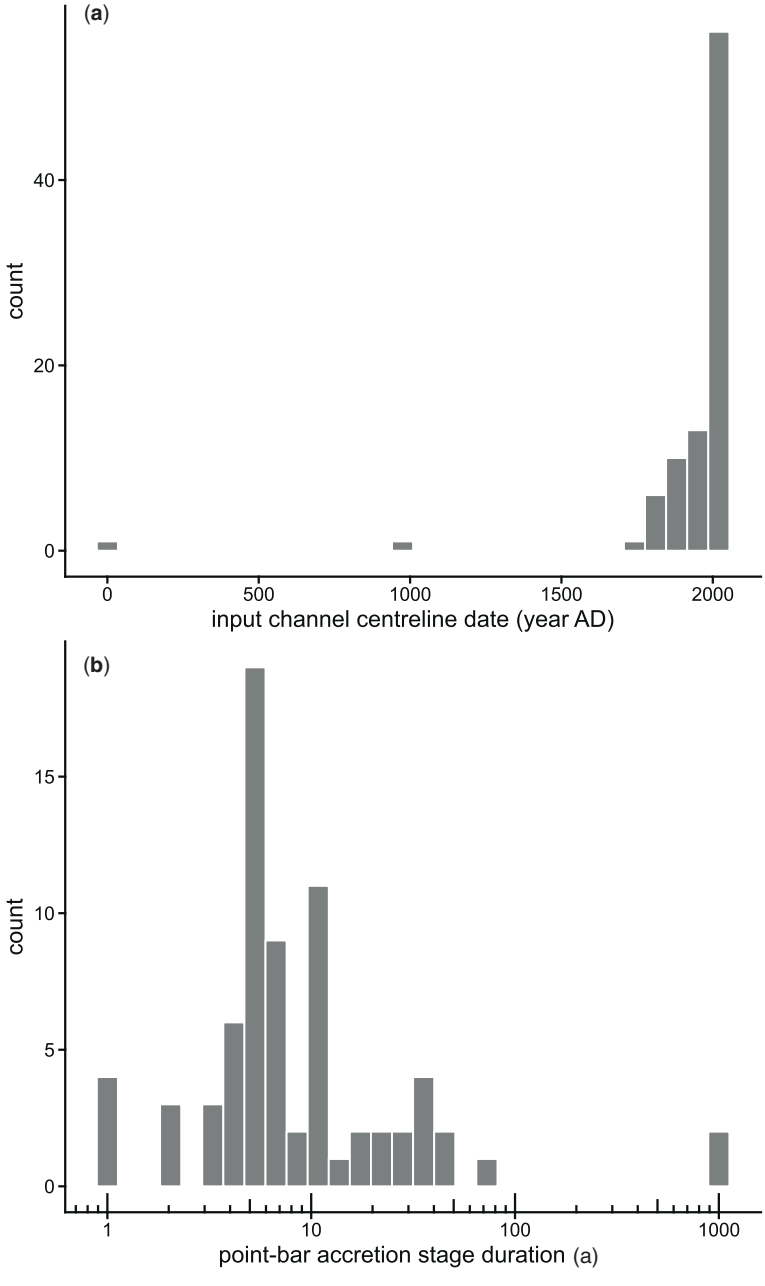

Fig. 3. Histograms of the temporal distribution of the input channel centrelines (**a**) and of the duration of point-bar accretion stages (**b**) of modelled meander-belt examples. Note that logarithmic scale is used in (b).

in channel bathymetry are not considered in the estimation (cf. Yan *et al.* 2021*b*). The model simulates erosion by shifting a channel centreline, and the present-day channel width is used for producing the visual outputs. The surface areas of accretion packages are calculated based on the reconstructed migration of channel centrelines, the position of which may differ from that of the position of channel thalwegs. This approach is preferred because the employed datasets only enable reconstruction of approximate channel centrelines; in any case, difference in the calculated preservation ratio may be

limited at the temporal and spatial scales of interest to this study.

Results

This section presents results relating to the following: (i) how the preservation ratio, the channel migration rate and the bar accretion rate change with the length of time over which they are considered, for different hierarchies of depositional products; and (ii) relationships between the preservation ratio and planform characteristics of meander belts and their accretion stages.

The planforms of 15 meander-belt examples modelled with PB-SAND are shown in Figure 4; these include nine examples of simple channel belts with no meander-bend cutoffs and six examples of complex channel belts with one or more bend cutoffs. They vary in size with changes of channel width from 6 to 963 m. Some meander belts appear to have evolved by dominant lateral migration and bend expansion, for example, *CB_1*, *CB_6*, *CB_12* and *CB_13*; other examples show dominant downstream migration and bend translation, e.g. *CB_3*, *CB_4*, *CB_8* and *CB_11*. The selected meander belts display bar-apex rotation varying between 3 to 13° on average over each accretion stage, with a minimum of 1° and a maximum of 30° for stage-forming accretion time steps.

The preservation ratio of all accumulated accretion stages and channel belts shows a very weak correlation with the time span of sedimentation, with a Pearson's correlation coefficient (r) of −0.228 and a p value of 0.021. The preservation ratio decreases overall across depositional hierarchies, from accretion stages to simple channel belts without cutoffs, to channel belts with cutoffs, with mean values of 0.993, 0.877 and 0.763, respectively (Fig. 5). The variability in preservation ratio is low for accretion stages ($N = 88$), with a standard deviation of 0.012; sediment preservation is more variable for both simple channel belts ($N = 7$) and channel belts with cutoffs ($N = 8$), with standard deviations of 0.136 and 0.117, respectively. A modest negative power-law relationship is seen between channel migration rate and the time span of sedimentation, with a coefficient of determination (r^2) of 0.346, and an exponent equal to −0.772 (Fig. 6a). A power-law relationship between the accretion rate and the time span of sedimentation yields a coefficient of determination of 0.377 and an exponent of −0.788 (Fig. 6c). Separate power-law relationships between channel migration rate and time for rivers of different orders of magnitude in size yield coefficients of determination of 0.782, 0.051 and 0.326 and exponents of −1.064, 0.138 and −0.442, for groups of rivers with channel width under 10 m, between 10 and 100 m, and between 100 and 1000 m, respectively (Fig. 6a). It is apparent nonetheless that the dataset is limited in size when broken down in the three orders of magnitude in river size, and this likely explains the weak fit, especially for rivers in the 10–100 m channel-width range. The overall trend suggests that separate power laws between migration rate and time may well describe the timescale dependency of accretion rates for rivers of different scales. Separate power-law relationships between mean accretion rate and time emerge if fitted to groups of examples that discriminate orders of magnitude in river size; these yield coefficients of determination of 0.801, 0.015 and 0.368 and exponents of −1.085, 0.077 and −0.490, for rivers with channels narrower than 10 m, between 10 to 100 m wide, and between 100 to 1000 m wide, respectively (Fig. 6c). Stronger positive power-law relationships exist between the channel width and both channel migration rate and accretion rate, with coefficients of determination of 0.655 and 0.629 and exponents of 1.705 and 1.660, respectively. There is a strong correlation between the channel migration rate and the bar accretion rate with a correlation coefficient of 0.995.

The relationships between the preservation ratio and the planform characteristics of the meander belts are assessed by integrating the results with those from the 34 examples modelled by Yan *et al.* (2021*a*) (Table 2; Figs 7 & 8); 49 case-study river reaches are therefore considered in total. There is no correlation between preservation ratio and average channel sinuosity (Pearson's $r = 0.046$, $p = 0.426$), circular mean of migration angle ($r = 0.000$, $p = 0.998$) or circular mean of bend rotation ($r = -0.001$, $p = 0.993$). No correlations exist between the same variables when these are considered separately for the different architectural hierarchies (accretion stages, simple channel belts without cutoffs and channel belts with cutoffs). However, the preservation ratio has a significant negative correlation with the circular standard deviation of migration angle across all architectural hierarchies ($r = -0.836$, $p < 0.001$). Modest negative correlations between the preservation ratio and the circular standard deviation of average migration angles are also found for simple channel belts ($r = -0.598$, $p < 0.001$), whereas weak correlations exist for accretion stages ($r = -0.190$, $p = 0.002$) and channel belts with cutoffs ($r = -0.058$, $p = 0.819$).

Discussion

Chronometrically constrained records of the evolution of meandering rivers enable evaluation of how channel-belt sediment preservation changes over time. This is achieved by building on results of Yan *et al.* (2021*a*), which were instead obtained by

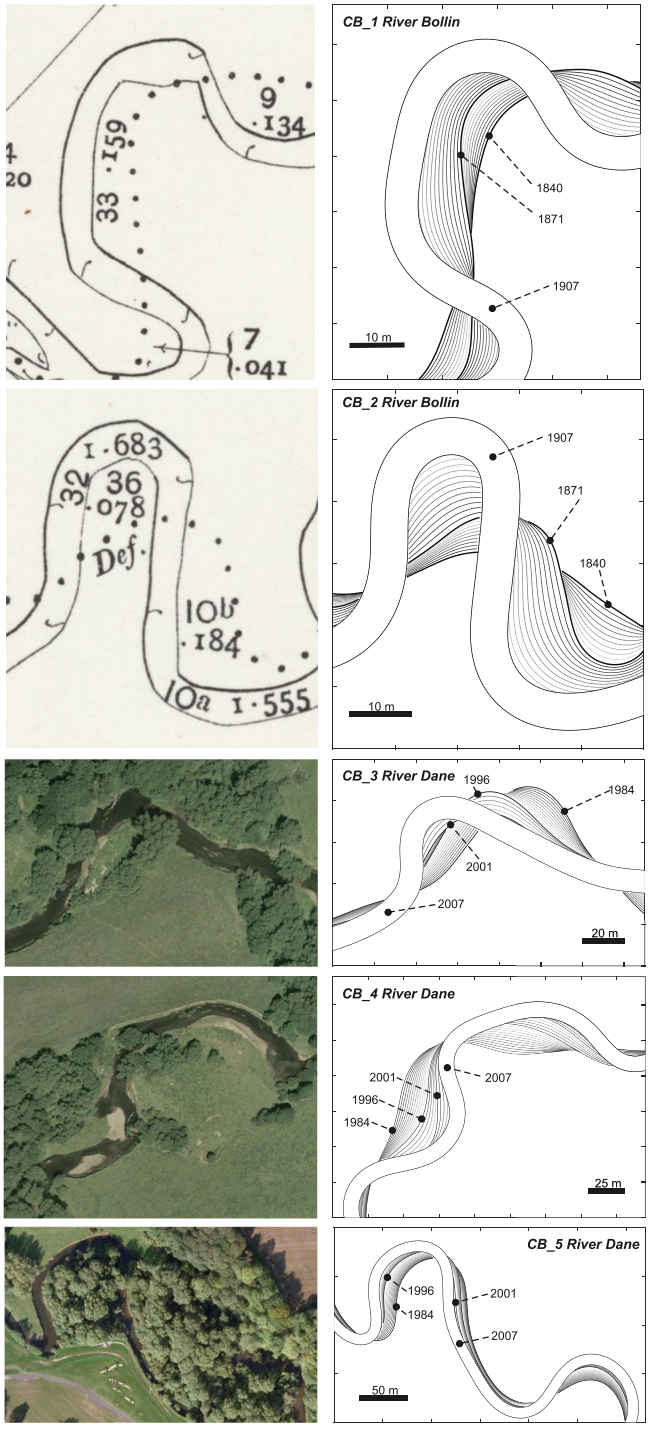

Fig. 4. Fifteen meander-belt cases portraying the planforms modelled using PB-SAND and the corresponding model outputs. Maps of *CB_1* and *CB_2* are from the 1909 Ordnance Survey sheet, Cheshire, UK, XXVIII.6 (mapped in 1907), in which dotted lines denote the boundary of civil parishes based on the position of earlier river courses. Ages of known river historical river channel positions are reported.

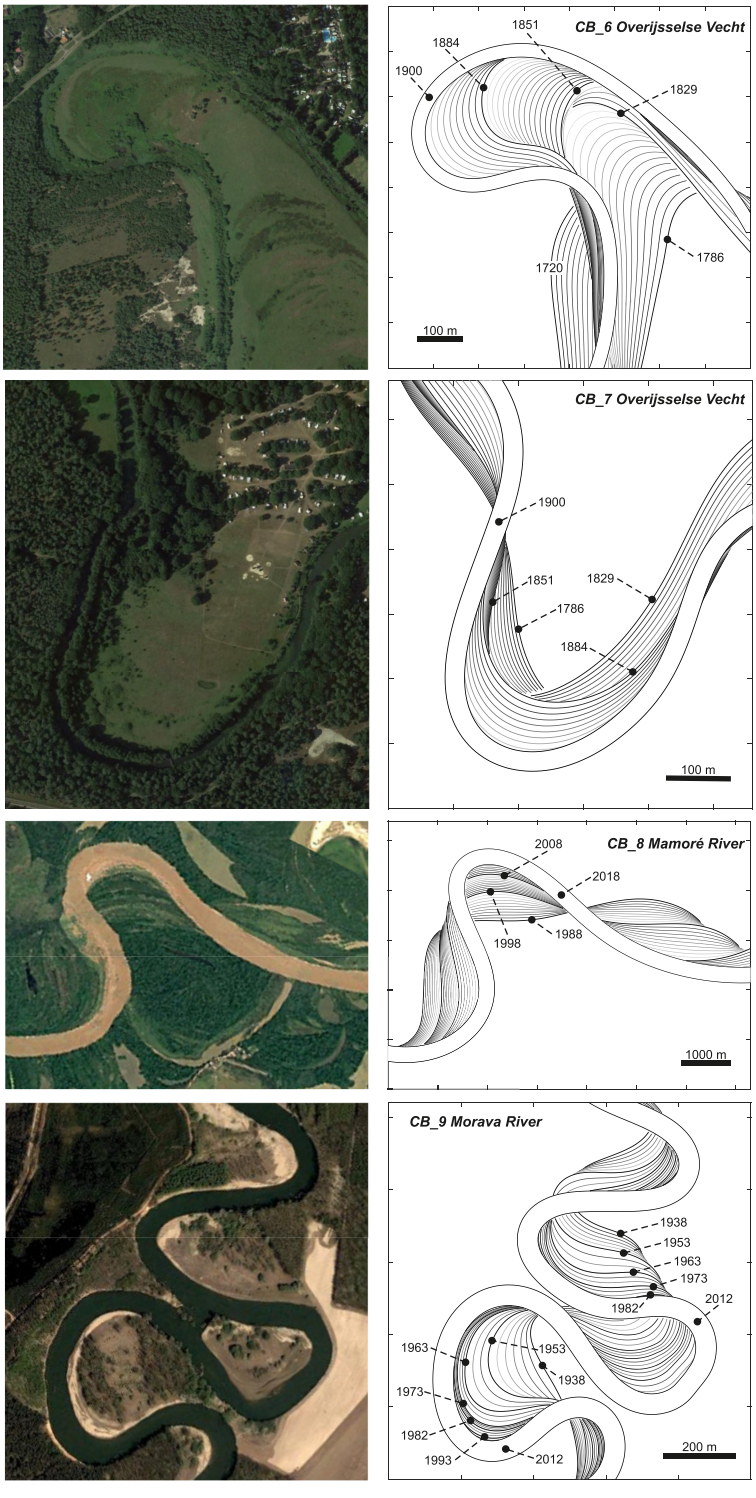

Fig. 4. *Continued.*

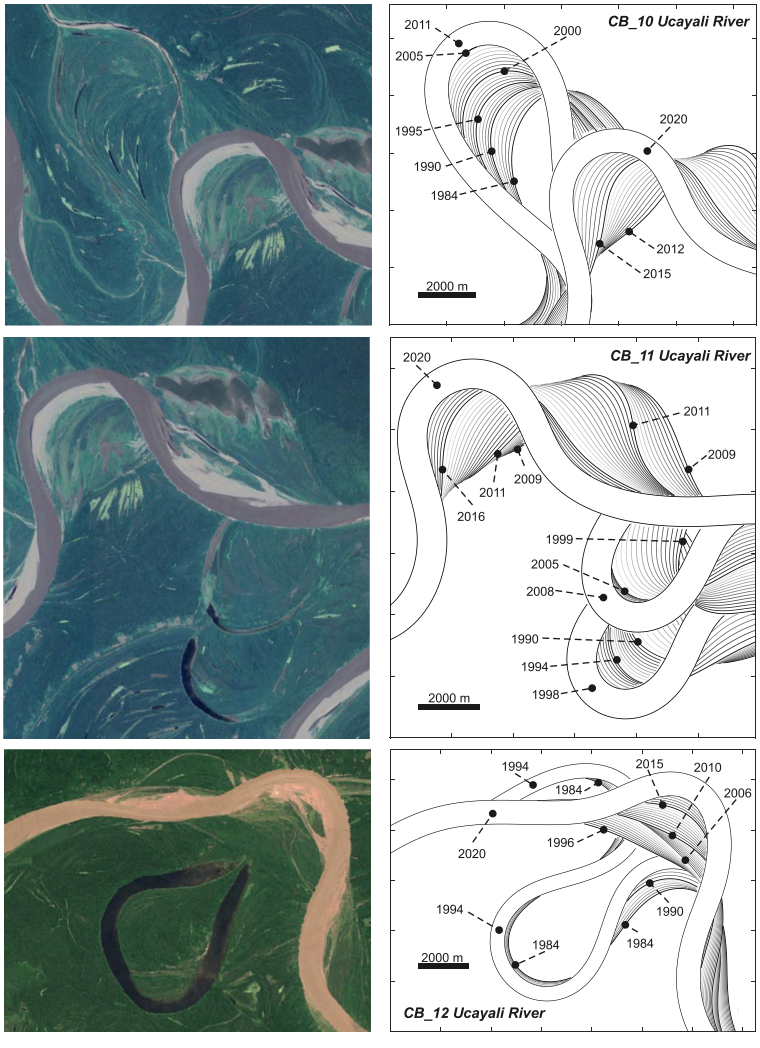

Fig. 4. *Continued.*

employing dimensionless time proxies. Such analysis is facilitated by the application of a numerical model for reconstructing temporal changes in channel-belt geomorphology. The results show that the preservation of meander-belt deposits decreases, but its variability increases, from individual accretion stages, through the development of simple channel belts, and ultimately to the evolution of complex channel belts with cutoffs (Fig. 5). For the three considered architectural hierarchies (accretion stages, simple channel belts and complex channel belts with cutoffs), sediment preservation is controlled by different predominant geomorphic factors that tend to operate at different timescales. Over durations of months to years, the frequency and the magnitude of intra-point-bar erosion vary greatly depending on the environmental and geomorphic controls and the associated meander-bend transformation styles (Fig. 5; Ielpi and Ghinassi 2014; Yan *et al.* 2021*a*, *b*). On a longer timescale, there are no apparent differences in preservation ratio between expansion-dominated and translation-dominated meander belts (Fig. 7a, b). This is due in part to the limited number of examples in which meander bends are dominated by translation for protracted time (Fig. 8a, b), and in part to the limited representativeness of the studied examples for the wide range of combinations of length in temporal evolution, rate of channel migration and style of morphodynamic change. Nonetheless, this also reflects, in part, how

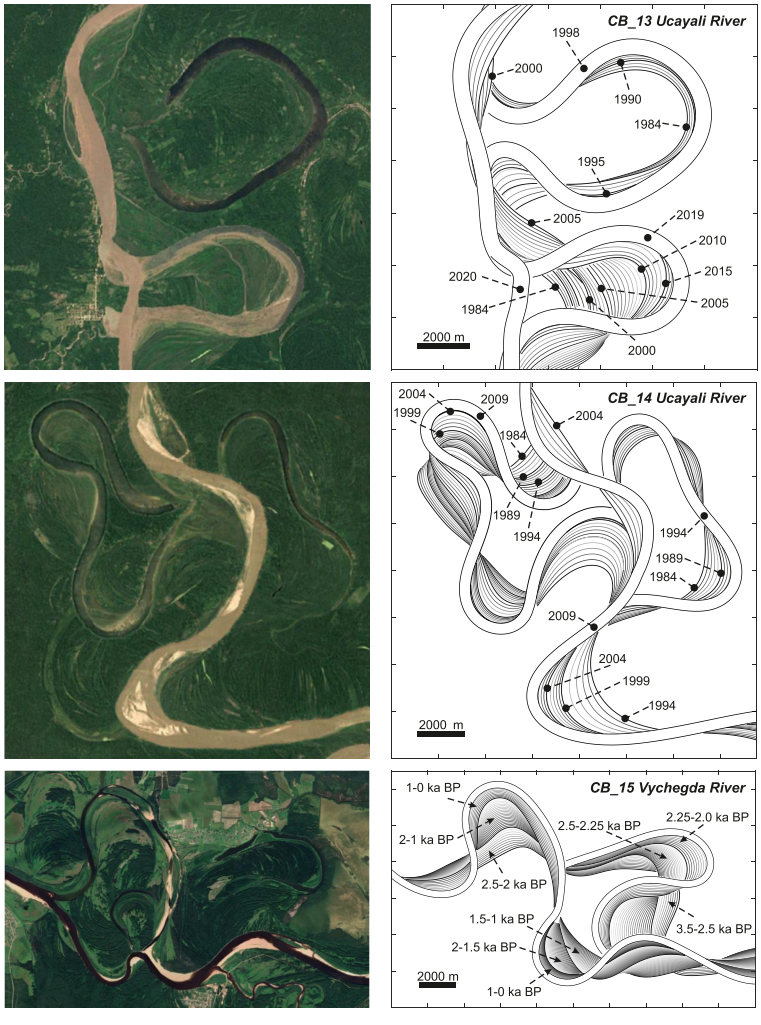

Fig. 4. *Continued.*

chute or neck cutoffs and the associated erosion of older bar deposits occur more commonly for expansion-dominated meander belts that are sufficiently mature (Schumm 1973; Camporeale *et al.* 2008; Schwenk and Foufoula-Georgiou 2016). Frequent changes in migration direction of meander bends can also cause repeated localized erosion of channel-belt deposits from earlier accretion stages and reduced sediment preservation; this is particularly significant where frequent toggling occurs between bend expansion and downstream translation (Johnston and Holbrook 2019). Meander-bend rotation can, furthermore, drive point-bar erosion in the vicinity of the outer banks of rotating apices (Ielpi and Ghinassi 2014; Strick *et al.* 2018), but it seems to play a less important role in controlling channel-belt preservation compared to the other meander-bend transformation styles (Yan *et al.* 2021*a*). This might reflect how (i) erosion caused by bar-apex rotations is relatively localized, and (ii) bar-apex rotation is prevalent in any fluvial meandering systems, such that its impact on preservation is therefore ubiquitous.

Yan *et al.* (2021*a*) showed that a single power-law relationship between point-bar accretion rate and time of sedimentation (cf. Sadler 1981; Pelletier and Turcotte 1997) fails to capture the way in which river morphodynamics appear to control sediment preservation, whereby different architectural hierarchies (i.e. pairs of accretion packages, accretion stages and meander belts) appear to follow distinct power-law relationships. In that study, all meander-

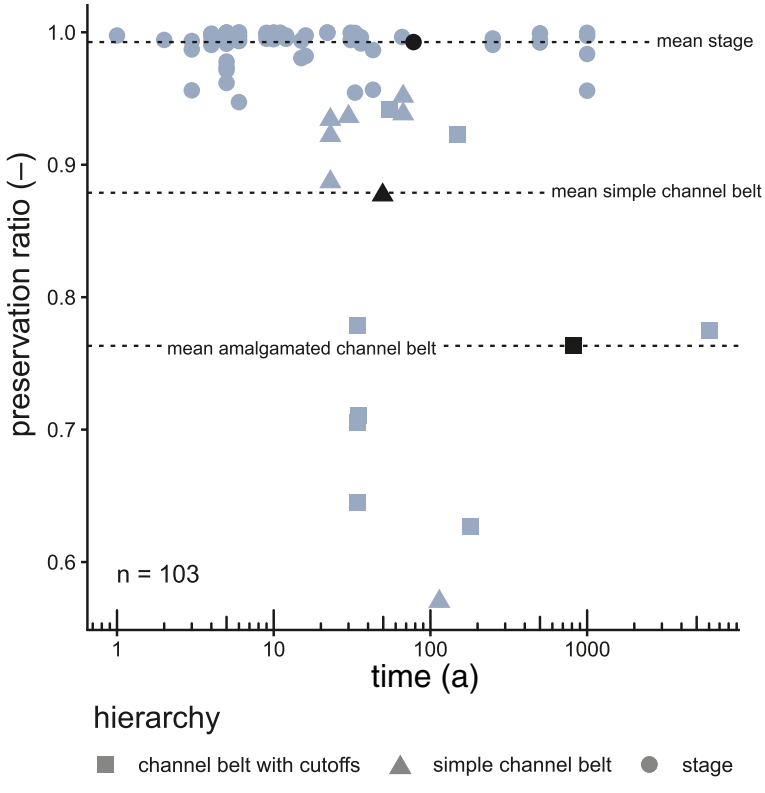

Fig. 5. Scatterplot of the relationship between preservation ratio and the time span of sedimentation, for different architectural hierarchies of the 15 modelled meander-belt cases.

belt examples were normalized in scale relative to the channel width, such that all modelled rivers were of the same idealized scale and therefore comparable. Furthermore, dimensionless proxies for temporal duration were employed that were based on the river migration area and the channel radii of curvature. Hence, one of the unknowns in the analyses was the degree to which a Sadler-type effect would be obfuscated by the dependency of accretion rates on river size and spatial scale. The results presented herein allow examination of whether these findings hold true for meandering channel belts associated with real temporal and spatial scales. Consistently with the findings by Yan *et al.* (2021*a*), the results indicate that a single power law does not effectively describe the relationship between the planform accretion rate of different architectural hierarchies. The size of a river, quantified here in terms of channel width, is directly related to rates of flow discharge and sediment transport and flux (Hooke 1980; Brice 1982; Hickin and Nanson 1984; Nanson and Hickin 1986; Lawler 1993; Hudson and Kesel 2000; Richard *et al.* 2005). As may be expected, the results indicate that separate power-law relationships may emerge between the accretion rate and the time of sedimentation for each order of magnitude of river size (channel width in the order of 10^0, 10^1 and 10^2 m). Within each group of examples associated with an order of magnitude in river size, the results seem to support the notion (Yan *et al.* 2021*a*) that different power-law relationships between accretion rate and time of sedimentation exist for different architectural hierarchies.

The importance of a space and time hierarchy in fluvial geomorphology has been appreciated since the 1960s (Schumm and Lichty 1965). River morphology has been recognized as scale-dependent in relation to a hierarchy of process events taking place at different temporal and spatial scale (e.g. from movement of a single grain, sediment transport in a reach, to erosion of a watershed) and expressed over different frequencies and magnitudes (De Boer 1992; Brunsden 2001). Our modelling results suggest that separate power-law relationships between meander-belt accretion rates and time exist for different architectural hierarchies and vary with system sizes, which is fundamentally controlled by a combination of morphological, geological and hydrological processes acting on different time and space scales (Couper 2004). Whereas meander-bend

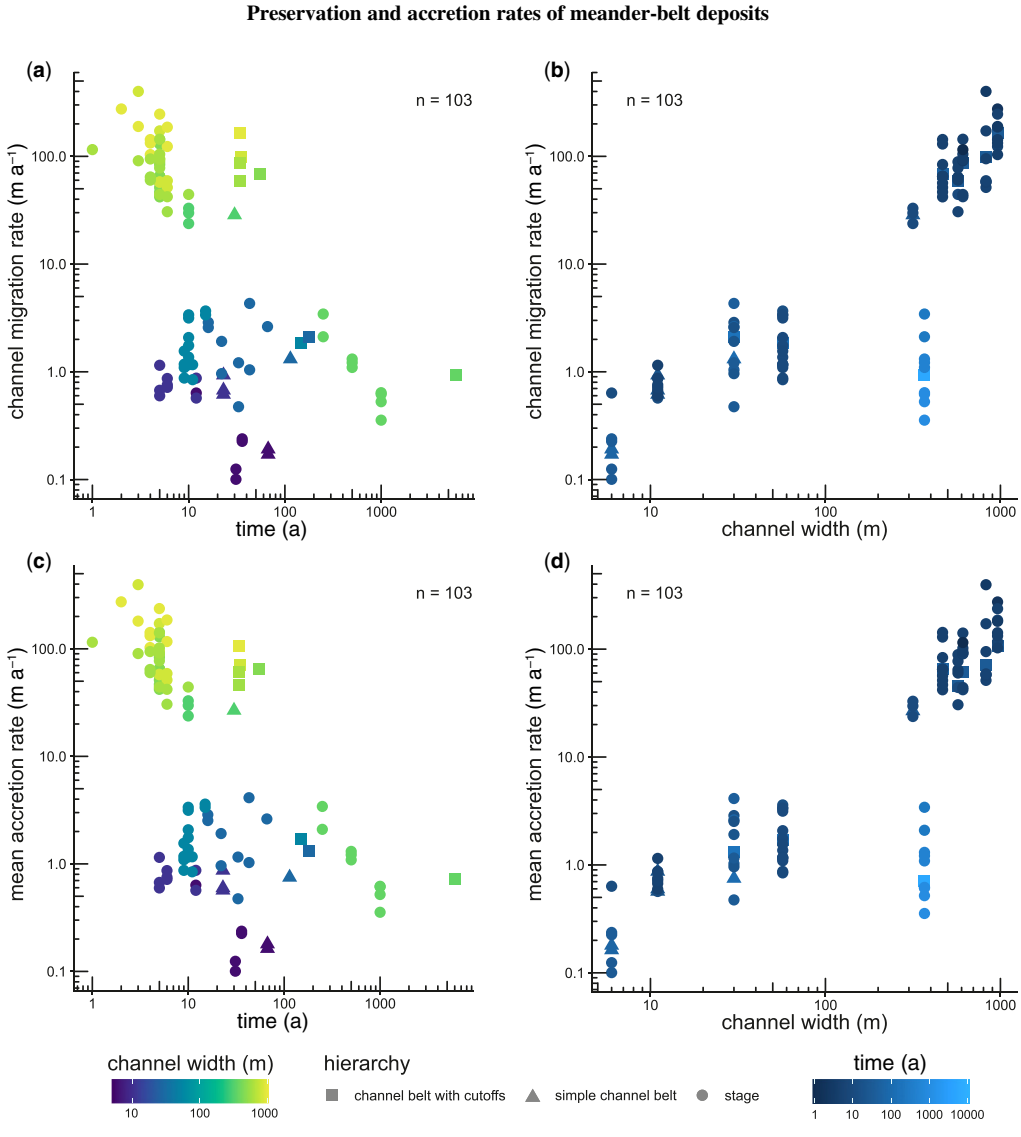

Fig. 6. Scatterplots of the relationships between channel migration rate and accretion rate v. the time span of sedimentation and channel width. Migration and accretion rates are in many cases very similar in magnitude, due to the relatively limited temporal lengths modelled.

Table 2. *Pearson's correlation coefficients* r *and their* p *values describing relationships between the preservation ratio and the planform characteristics of meander belts for different architectural hierarchies*

	Sinuosity		Migration angle circular mean		Bend rotation circular mean		Circular standard deviation migration angle	
	r	*p*	*r*	*p*	*r*	*p*	*r*	*p*
All	0.046	0.426	0.000	0.998	−0.001	0.993	−0.836	<0.001
Simple channel belts	0.260	0.158	0.061	0.743	−0.067	0.720	−0.598	<0.001
channel belts with cutoffs	0.407	0.093	0.110	0.663	−0.019	0.940	−0.058	0.819
Accretion stage	0.018	0.774	−0.067	0.285	−0.042	0.498	−0.190	0.002

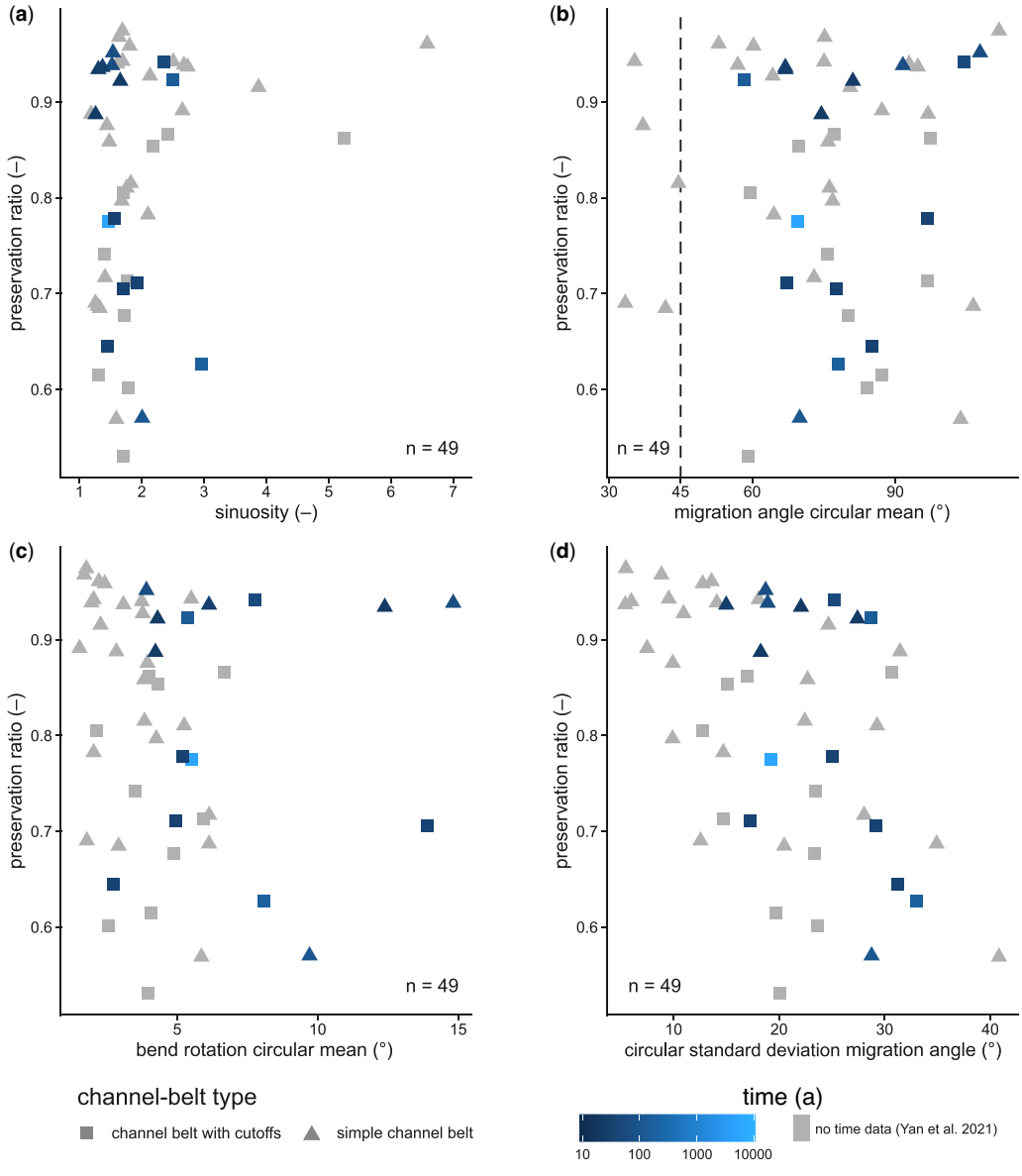

Fig. 7. Relationships between preservation ratio and planform characteristics of meander belts. See text and Figure 1a for definitions of planform-evolution descriptors.

rotations happen steadily in meandering channels, major bend cut-off events only occur when a threshold is reached, such as at a time of critical bend tightening or due to high-magnitude, low-frequency floods (Knox 2001; Brunsden 2001). Morphological changes are typically gradual processes and exhibit hysteresis. Bend cutoff serves as a geomorphic threshold that drives the system towards a new quasi-equilibrium state, which may potentially trigger further cutoffs along stream (Schumm 1973; Camporeale *et al.* 2008; Schwenk and Foufoula-Georgiou 2016). The influence of neck or chute cutoff events on bar preservation becomes important for channel belts that have reached a certain maturity, and results in the variation of channel-belt accretion rates for rivers of different sizes.

However, temporal variations in sediment preservation appear to only exert a limited control on

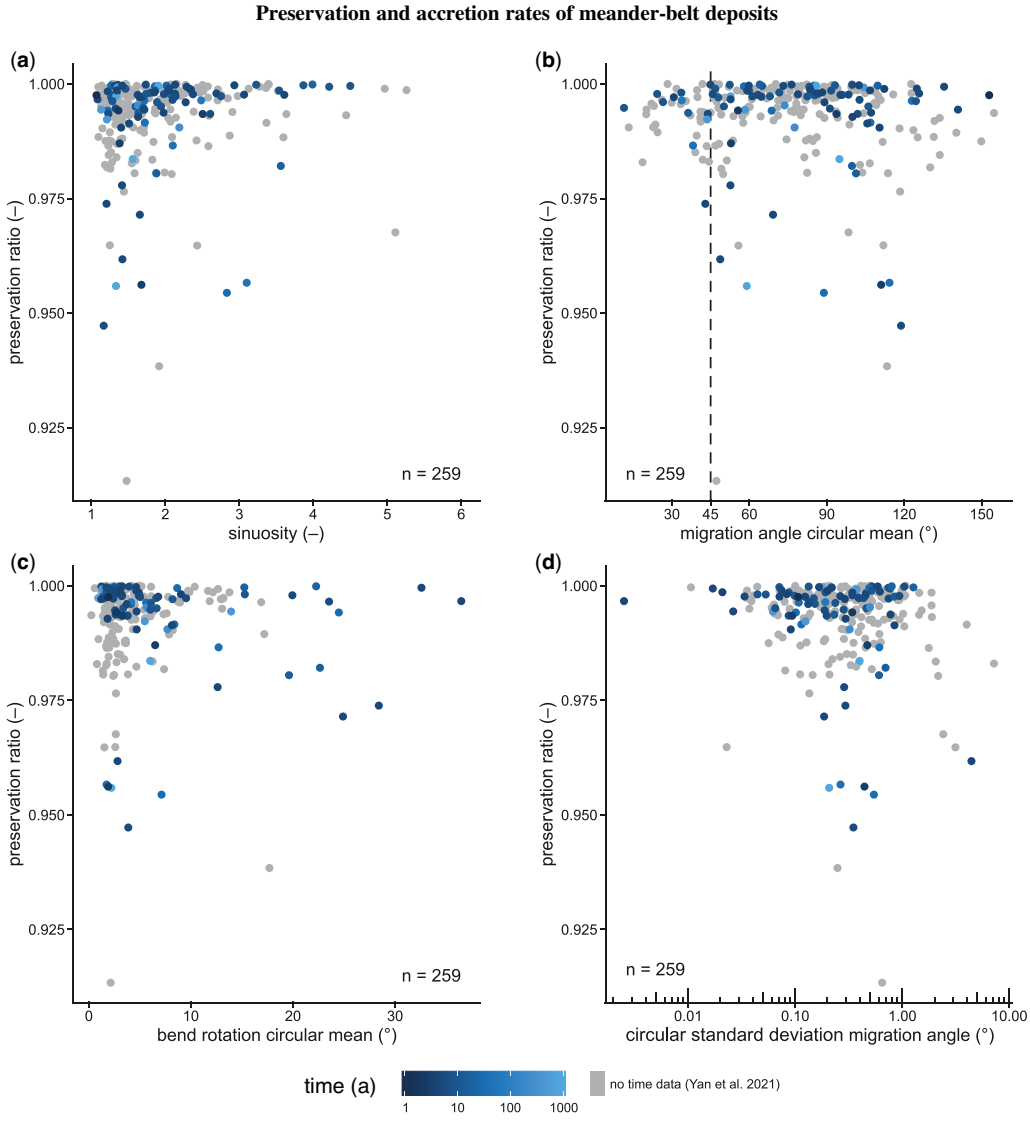

Fig. 8. Relationships between preservation ratio and planform characteristics of accretion stages of meander-belt deposits. See text and Figure 1a for definitions of planform-evolution descriptors.

the emergence of a Sadler-type relationship describing the dependency of accretion rates with time, and accretion rates are seen to vary in concert with channel migration rates across the examined examples. As the bar accretion rate is inherently related to the channel migration rate, it is significant that (i) both rates show a similar negative correlation with the time of sedimentation (Fig. 6a, c), and that (ii) power laws can describe the decays with time of both rates if examples grouped by orders of magnitude in river size are separately considered. It is apparent that the observed variations in meander-belt accretion rates with time are more strongly controlled by the rates of channel migration, rather than the temporal variations in sediment preservation due to the increased likelihood of erosion over longer time spans. In this perspective, at the temporal scales considered in this work, the observed dependency of meander-belt accretion rates on time does not appear as the expression of a true Sadler-type effect. It then becomes important to establish possible explanations of the observed relationships between channel migration rates and time for rivers of given magnitude in size, and particularly whether they are merely apparent trends (cf. Schook *et al.* 2017). Given that the evolutions

of almost all studied examples are modelled up to the present day, it is possible that the decrease in migration rate with time is a result of some systematic progressive acceleration of river mobility through time. However, this idea contradicts the notion of a general decrease in channel migration rate through the Holocene (Candel *et al.* 2018). It is perhaps more likely that the trend reflects how the reconstructed area over which a river migrated during a defined timespan varies with the number of centrelines employed to constrain that reconstruction. The average duration between two consecutive control centrelines tends to be longer for older river histories, for which temporal constraints are sparser, resulting in highly skewed distributions of centreline ages and stage durations (Fig. 2). Channel adjustments and bend transformations, as well as sediment erosion taking place below the available temporal resolution, are not captured by the linear interpolation operated by the model. This then leads to an underestimation of the channel migration area and migration rate, and to an overestimation of the preservation ratio. As the interval between input trajectories become larger, the channel migration rate is increasingly underestimated. A possible additional cause for the observed inverse correlation between time and migration rate, and hence accretion rate, lies in the inherent bias of the chosen examples of meander-belt evolution. It is likely that the selected examples characterized by development times that are on average shorter (decadal scale) tend to be characterized by more rapid rates of channel migration, because marked changes in planform morphology must have occurred for the examples to be considered significant enough for inclusion in this study. It is also plausible that examples that record comparatively longer histories (centennial to millennial scales) must have experienced rates of geomorphic change that were sufficiently slow to enable their reconstruction from historical records. It is, therefore, likely that the form of dependency of meander-belt accretion rates on time documented here and in Yan *et al.* (2021*b*) is due in part to (i) intrinsic limitations of the chosen approach when applied to examples that vary with respect to the density of temporal constraints, and (ii) bias due to how the necessary dataset is assembled. Both factors represent issues that will affect other similar studies, be they undertaken with a similar numerical modelling approach or other deterministic planform reconstructions.

Conclusions

Fifteen meander-belt examples with known temporal evolution have been reconstructed with a forward stratigraphic model to evaluate how sediment preservation and accretion rates of fluvial meander-belt deposits change as the time of sedimentation increases for different hierarchies of sedimentary products including (i) accretion stages, (ii) simple meander-belt segments without bend cutoffs and (iii) complex meander-belt segments with one or multiple cutoffs. The results support and augment findings by Yan *et al.* (2021*a*). Separate power-law relationships between accretion rate and time of sedimentation emerge for different architectural hierarchies. Different power-law relationships also seem to exist for the depositional products of rivers of different sizes, described herein by channel widths in the order of 10^0, 10^1 and 10^2 m. Nonetheless, the importance of sediment preservation in determining relationships between accretion rates and time appears to be secondary. Instead, systematic variations in accretion rates with time appear to be overwhelmingly a reflection of apparent variations in river migration rates with time. Explanations for this can be found in: (i) intrinsic limitations posed by the application of the algorithm to meander belts with variable temporal resolution; (ii) bias in the selected meander-belt examples. These findings should be taken into account when applying comparable numerical approaches in the assessment of river migration rates, channel-belt accretion rates and sediment preservation over variable time windows (Schwenk *et al.* 2017; Boothroyd *et al.* 2021; Jarriel *et al.* 2021).

Acknowledgements We thank Alvise Finotello and Paul Durkin for their invitation to contribute this paper, and Liz Hajek and two anonymous reviewers for their constructive comments, which have improved the manuscript greatly. We also thank CNOOC International, Canada (formerly Nexen), for financial support for development of PB-SAND, and FRG-ERG-SMRG sponsors (AkerBP, Areva [now Orano], BHP, Cairn India [Vedanta], Chevron, CNOOC International, ConocoPhillips, Equinor, Murphy Oil, Occidental, Saudi Aramco, Shell, Tullow Oil, Woodside, and YPF) and their partner Petrotechnical Data Systems for financial support of the research group.

Competing interests The authors declare that they have no known competing financial interests or personal relationships that could have appeared to influence the work reported in this paper.

Author contributions **NY**: conceptualization (lead), data curation (lead), formal analysis (lead), funding acquisition (supporting), methodology (lead), software (lead), visualization (lead), writing – original draft (lead), writing – review & editing (lead); **LC**: conceptualization (supporting), formal analysis (supporting), funding acquisition (supporting), methodology (supporting), visualization (supporting), writing – original draft (supporting), writing – review & editing (supporting); **NPM**: funding acquisition

(lead), writing – original draft (supporting), writing – review & editing (supporting).

Funding This research is funded by the Fluvial, Eolian & Shallow-Marine Research Group, University of Leeds.

Data availability Data are available from the corresponding author on reasonable request.

References

Ager, D.V. 1993. *The Nature of the Stratigraphical Record*, 3rd edn. Wiley–Blackwell.

Barrell, J. 1917. Rhythms and the measurements of geologic time. *Geological Society of America Bulletin*, **28**, 745–904, https://doi.org/10.1130/GSAB-28-745

Boothroyd, R.J., Williams, R.D., Hoey, T.B., Tolentino, P.L.M. and Yang, X. 2021. National-scale assessment of decadal river migration at critical bridge infrastructure in the Philippines. *Science of the Total Environment*, **768**, 144460, https://doi.org/10.1016/j.scitotenv.2020.144460

Brice, J.C. 1982. *Stream Channel Stability Assessment*. Federal Highway Administration, United States.

Brunsden, D. 2001. A critical assessment of the sensitivity concept in geomorphology. *Catena*, **42**, 99–123, https://doi.org/10.1016/S0341-8162(00)00134-X

Camporeale, C., Perucca, E. and Ridolfi, L. 2008. Significance of cutoff in meandering river dynamics. *Journal of Geophysical Research: Earth Surface*, **113**, 2006JF000694, https://doi.org/10.1029/2006JF000694

Candel, J.H.J., Kleinhans, M.G., Makaske, B., Hoek, W.Z., Quik, C. and Wallinga, J. 2018. Late Holocene channel pattern change from laterally stable to meandering – a palaeohydrological reconstruction. *Earth Surface Dynamics*, **6**, 723–741, https://doi.org/10.5194/esurf-6-723-2018

Couper, P.R. 2004. Space and time in river bank erosion research: a review. *Area*, **36**, 387–403, https://doi.org/10.1111/j.0004-0894.2004.00239.x

Daniel, J.F. 1971. *Channel Movement of Meandering Indiana Streams*. US Government Printing Office.

De Boer, D.H. 1992. Hierarchies and spatial scale in process geomorphology: a review. *Geomorphology*, **4**, 303–318, https://doi.org/10.1016/0169-555X(92)90026-K

Dott, R., Jr. 1996. Episodic event deposits v. stratigraphic sequences – shall the twain never meet? *Sedimentary Geology*, **104**, 243–247, https://doi.org/10.1016/0037-0738(95)00131-X

Durkin, P.R., Hubbard, S.M., Holbrook, J. and Boyd, R. 2018. Evolution of fluvial meander-belt deposits and implications for the completeness of the stratigraphic record. *Geological Society of America Bulletin*, **130**, 721–739, https://doi.org/10.1130/B31699.1

Durkin, P.R., Hubbard, S.M., Smith, D.G. and Leckie, D.A. 2019. Predicting heterogeneity in meandering fluvial and tidal-fluvial deposits: The point bar to counter point bar transition. *In*: Ghinassi, M., Mountney, N., Colombera, L. and Reesink, A.J. (eds) *Meandering Rivers and Their Depositional Record*. John Wiley and Sons, 231–250,

Friend, P. and Sinha, R. 1993. Braiding and meandering parameters. *Geological Society, London, Special Publications*, **75**, 105–111, https://doi.org/10.1144/GSL.SP.1993.075.01.05

Ghinassi, M. and Ielpi, A. 2015. Stratal architecture and morphodynamics of downstream-migrating fluvial point bars (Jurassic Scalby Formation, UK). *Journal of Sedimentary Research*, **85**, 1123–1137, https://doi.org/10.2110/jsr.2015.74

Ghinassi, M., Nemec, W., Aldinucci, M., Nehyba, S., Özaksoy, V. and Fidolini, F. 2014. Plan-form evolution of ancient meandering rivers reconstructed from longitudinal outcrop sections. *Sedimentology*, **61**, 952–977, https://doi.org/10.1111/sed.12081

Ghinassi, M., Ielpi, A., Aldinucci, M. and Fustic, M. 2016. Downstream-migrating fluvial point bars in the rock record. *Sedimentary Geology*, **334**, 66–96, https://doi.org/10.1016/j.sedgeo.2016.01.005

Hagstrom, C.A., Hubbard, S.M., Leckie, D.A. and Durkin, P.R. 2019. The effects of accretion-package geometry on lithofacies distribution in point-bar deposits. *Journal of Sedimentary Research*, **89**, 381–398, https://doi.org/10.2110/jsr.2019.23

Hickin, E.J. and Nanson, G.C. 1984. Lateral migration rates of river bends. *Journal of Hydraulic Engineering*, **110**, 1557–1567, https://doi.org/10.1061/(ASCE)0733-9429(1984)110:11(1557)

Hooke, J.M. 1995. River channel adjustment to meander cutoffs on the River Bollin and River Dane, northwest England. *Geomorphology*, **14**, 235–253, https://doi.org/10.1016/0169-555X(95)00110-Q

Hooke, J.M. 1980. Magnitude and distribution of rates of river bank erosion. *Earth Surface Processes*, **5**, 143–157, https://doi.org/10.1002/esp.3760050205

Hooke, J.M. 2004. Cutoffs galore!: occurrence and causes of multiple cutoffs on a meandering river. *Geomorphology*, **61**, 225–238, https://doi.org/10.1016/j.geomorph.2003.12.006

Hooke, J.M. and Yorke, L. 2010. Rates, distributions and mechanisms of change in meander morphology over decadal timescales, River Dane, UK. *Earth Surface Processes and Landforms*, **35**, 1601–1614, https://doi.org/10.1002/esp.2079

Hudson, P.F. and Kesel, R.H. 2000. Channel migration and meander-bend curvature in the lower Mississippi River prior to major human modification. *Geology*, **28**, 531–534, https://doi.org/10.1130/0091-7613(2000)28<531:CMAMCI>2.0.CO;2

Ielpi, A. and Ghinassi, M. 2014. Planform architecture, stratigraphic signature and morphodynamics of an exhumed Jurassic meander plain (Scalby Formation, Yorkshire, UK). *Sedimentology*, **61**, 1923–1960, https://doi.org/10.1111/sed.12122

Jarriel, T., Swartz, J. and Passalacqua, P. 2021. Global rates and patterns of channel migration in river deltas. *Proceedings of the National Academy of Sciences*, **118**, e2103178118, https://doi.org/10.1073/pnas.2103178118

Johnston, S. and Holbrook, J. 2019. Toggling between expansion and translation: the generation of a muddy-normal point bar with an earthquake imprint. *In*: Ghinassi, M., Mountney, N., Colombera, L. and Reesink, A.J. (eds) *Meandering Rivers and Their Depositional Record*. John Wiley and Sons, 47–80.

Karmanov, V., Chernov, A., Zaretskaya, N., Panin, A. and Volokitin, A. 2013. Paleochannel studies in archaeology: the case of the Vychegda River, Northeastern European Russia. *Archaeology, Ethnology and Anthropology of Eurasia*, **41**, 83–93, https://doi.org/10.1016/j.aeae.2013.11.008

Knox, J.C. 2001. Agricultural influence on landscape sensitivity in the Upper Mississippi River Valley. *Catena*, **42**, 193–224, https://doi.org/10.1016/S0341-8162(00)00138-7

Labrecque, P.A., Hubbard, S.M., Jensen, J.L. and Nielsen, H. 2011. Sedimentology and stratigraphic architecture of a point bar deposit, Lower Cretaceous McMurray Formation, Alberta, Canada. *Bulletin of Canadian Petroleum Geology*, **59**, 147–171, https://doi.org/10.2113/gscpgbull.59.2.147

Lawler, D.M. 1993. The measurement of river bank erosion and lateral channel change: a review. *Earth Surface Processes and Landforms*, **18**, 777–821, https://doi.org/10.1002/esp.3290180905

Miall, A.D. 2015. Updating uniformitarianism: stratigraphy as just a set of 'frozen accidents'. *Geological Society, London, Special Publications*, **404**, 11–36, https://doi.org/10.1144/SP404.4

Nanson, G.C. and Hickin, E.J. 1986. A statistical analysis of bank erosion and channel migration in western Canada. *Geological Society of America Bulletin*, **97**, 497–504, https://doi.org/10.1130/0016-7606(1986)97<497:ASAOBE>2.0.CO;2

Ondruch, J. and Máčka, Z. 2015. Response of lateral channel dynamics of a lowland meandering river to engineering-derived adjustments-an example of the Morava River (Czech Republic). *Open Geosciences*, **7**, https://doi.org/10.1515/geo-2015-0047

Pelletier, J.D. and Turcotte, D.L. 1997. Synthetic stratigraphy with a stochastic diffusion model of fluvial sedimentation. *Journal of Sedimentary Research*, **67**, 1060–1067.

Quik, C. and Wallinga, J. 2018. Reconstructing lateral migration rates in meandering systems–a novel Bayesian approach combining optically stimulated luminescence (OSL) dating and historical maps. *Earth Surface Dynamics*, **6**, 705–721, https://doi.org/10.5194/esurf-6-705-2018

Richard, G.A., Julien, P.Y. and Baird, D.C. 2005. Statistical analysis of lateral migration of the Rio Grande, New Mexico. *Geomorphology*, **71**, 139–155, https://doi.org/10.1016/j.geomorph.2004.07.013

Russell, C.E., Mountney, N.P., Hodgson, D.M. and Colombera, L. 2019. A novel approach for prediction of lithological heterogeneity in fluvial point-bar deposits from analysis of meander morphology and scroll-bar pattern. *In*: Ghinassi, M., Mountney, N., Colombera, L. and Reesink, A.J. (eds) *Meandering Rivers and Their Depositional Record*. John Wiley and Sons, 385–418.

Sadler, P.M. 1981. Sediment accumulation rates and the completeness of stratigraphic sections. *The Journal of Geology*, **89**, 569–584, https://doi.org/10.1086/628623

Sadler, P.M. and Strauss, D.J. 1990. Estimation of completeness of stratigraphical sections using empirical data and theoretical models. *Journal of the Geological Society, London*, **147**, 471–485, https://doi.org/10.1144/gsjgs.147.3.0471

Schook, D.M., Rathburn, S.L., Friedman, J.M. and Wolf, J.M. 2017. A 184-year record of river meander migration from tree rings, aerial imagery, and cross sections. *Geomorphology*, **293**, 227–239, https://doi.org/10.1016/j.geomorph.2017.06.001

Schumm, S. 1973. Geomorphic thresholds and complex response of drainage systems. *Fluvial Geomorphology*, **6**, 69–85.

Schumm, S.A. and Lichty, R.W. 1965. Time, space and causality in geomorphology. *American Journal of Science*, **263**, 110–119.

Schwenk, J. and Foufoula-Georgiou, E. 2016. Meander cutoffs nonlocally accelerate upstream and downstream migration and channel widening. *Geophysical Research Letters*, **43**, 12437–12445, https://doi.org/10.1002/2016GL071670

Schwenk, J., Khandelwal, A., Fratkin, M., Kumar, V. and Foufoula-Georgiou, E. 2017. High spatiotemporal resolution of river planform dynamics from Landsat: the RivMAP toolbox and results from the Ucayali River. *Earth and Space Science*, **4**, 46–75, https://doi.org/10.1002/2016EA000196

Smith, D.G., Hubbard, S.M., Leckie, D.A. and Fustic, M. 2009. Counter point bar deposits: lithofacies and reservoir significance in the meandering modern Peace River and ancient McMurray Formation, Alberta, Canada. *Sedimentology*, **56**, 1655–1669, https://doi.org/10.1111/j.1365-3091.2009.01050.x

Smith, D.G., Hubbard, S.M., Lavigne, J.R., Leckie, D.A. and Fustic, M. 2011. Stratigraphy of counter-point-bar and eddy-accretion deposits in low-energy meander belts of the Peace-Athabasca Delta, Northeast Alberta, Canada. *In*: Davidson, S.K., Leleu, S. and North, C.P. (eds) *From River to Rock Record: The Preservation of Fluvial Sediments and Their Subsequent Interpretation*. Society for Sedimentary Geology Special Publication, SEPM – Society for Sedimentary Geology, Tulsa, **97**, 143–152.

Strick, R.J.P., Ashworth, P.J., Awcock, G. and Lewin, J. 2018. Morphology and spacing of river meander scrolls. *Geomorphology*, **310**, 57–68, https://doi.org/10.1016/j.geomorph.2018.03.005

Sylvester, Z., Durkin, P., Hubbard, S. and Mohrig, D. 2021. Autogenic translation and counter point bar deposition in meandering rivers. *Geological Society of America Bulletin*, **133**, 2439–2456, https://doi.org/10.1130/B35829.1

Viero, D.P., Dubon, S.L. and Lanzoni, S. 2018. Chute cutoffs in meandering rivers: formative mechanisms and hydrodynamic forcing. *In*: Ghinassi, M., Mountney, N., Colombera, L. and Reesink, A.J. (eds) *Meandering Rivers and Their Depositional Record*. John Wiley and Sons, 201–229.

Walcker, R., Corenblit, D., Julien, F., Martinez, J.-M. and Steiger, J. 2021. Contribution of meandering rivers to natural carbon fluxes: evidence from the Ucayali River, Peruvian Amazonia. *Science of the Total Environment*, **776**, 146056, https://doi.org/10.1016/j.scitotenv.2021.146056

Willis, B.J. and Sech, R.P. 2019. Emergent facies patterns within fluvial channel belts. *In*: Ghinassi, M., Mountney, N., Colombera, L. and Reesink, A.J. (eds) *Meandering Rivers and Their Depositional Record*. John Wiley and Sons, 509–542.

Yan, N., Mountney, N.P., Colombera, L. and Dorrell, R.M. 2017. A 3D forward stratigraphic model of fluvial meander-bend evolution for prediction of point-bar lithofacies architecture. *Computers & Geosciences*, **105**, 65–80, https://doi.org/10.1016/j.cageo.2017.04.012

Yan, N., Colombera, L. and Mountney, N.P. 2021*a*. Evaluation of morphodynamic controls on the preservation of fluvial meander-belt deposits. *Geophysical Research Letters*, **48**, e2021GL094622, https://doi.org/10.1029/2021GL094622

Yan, N., Colombera, L. and Mountney, N.P. 2021*b*. Controls on fluvial meander-belt thickness and sand distribution: insights from forward stratigraphic modelling. *Sedimentology*, **68**, 1831–1860, https://doi.org/10.1111/sed.12830